ELSEVIER

Journal of Organometallic Chemistry 527 (1997) 247–258

Journal of Organometallic Chemistry

Diiron σ–π alkenyl complexes: crystal structures of *cis*-[$Fe_2(CO)_4(\mu$-$RC{=}CH_2)(\mu$-$PPh_2)(\mu$-dppm)], (R = Ph, CH_2OH), *trans*-[$Fe_2(CO)_4(\mu$-$HC{=}CHPh)(\mu$-$PPh_2)(\mu$-dppm)] and the α,β-unsaturated acyl complex *trans*-[$Fe_2(CO)_4\{\mu$-$O{=}C{-}C(Ph){=}CH_2\}(\mu$-$PCy_2)(\mu$-dppm)]

Graeme Hogarth *, Mark H. Lavender, Khalid Shukri

Chemistry Department, University College London, 20 Gordon Street, London WC1H 0AJ, UK

Received 12 June 1996

Abstract

Insertion of phenylethyne into *cis*-[$Fe_2(CO)_4(\mu$-H)(μ-CO)(μ-PPh_2)(μ-dppm)] **1a** affords isomers *cis*-[$Fe_2(CO)_4(\mu$-$PhC{=}CH_2$)(μ-PPh_2)(μ-dppm)] **2a** and *trans*-[$Fe_2(CO)_4(\mu$-$HC{=}CHPh$)(μ-PPh_2)(μ-dppm)] **2b** which differ in both the regioselectivity of the alkyne insertion (α and β) and the relative orientations of the phosphido and diphosphine ligands (*cis* and *trans*) respectively. In contrast, reaction with *trans*-[$Fe_2(CO)_4(\mu$-H)(μ-CO)(μ-PCy_2)(μ-dppm)] **1b** appears to give only the α-substituted product *trans*-[$Fe_2(CO)_4(\mu$-$PhC{=}CH_2$)(μ-PCy_2)(μ-dppm)] **3a**, however, thermolysis of the crude reaction mixture leads to the low yield isolation of the α,β-unsaturated acyl complex *trans*-[$Fe_2(CO)_4\{\mu$-$O{=}C{-}C(Ph){=}CH_2\}(\mu$-$PCy_2)(\mu$-dppm)] **4**, formally resulting from CO insertion into the unidentified β-substituted isomer. Reaction of **1a** with propargyl alcohol affords chromatographically separable isomers *cis*-[$Fe_2(CO)_4\{\mu$-$C(CH_2OH){=}CH_2\}(\mu$-$PPh_2)(\mu$-dppm)] **5a** and *trans*-[$Fe_2(CO)_4(\mu$-$HC{=}CH(CH_2OH))(\mu$-$PPh_2)(\mu$-dppm)] **5b**, while with **1b** an inseparable mixture of *trans*-[$Fe_2(CO)_4\{\mu$-$C(CH_2OH){=}CH_2\}(\mu$-$PCy_2)(\mu$-dppm)] **6a** and *trans*-[$Fe_2(CO)_4(\mu$-$HC{=}CH(CH_2OH))(\mu$-$PCy_2)(\mu$-dppm)] **6b** results. Complexes **2a**, **2b**, **4** and **5a** have been characterised by single crystal X-ray diffraction analyses. All μ-alkenyl complexes undergo 'windshield-wiper' fluxionality on the NMR timescale, with free energies of activation varying dramatically, an effect which can be correlated with the mode of binding of the alkenyl ligand in the solid state.

Keywords: Diiron; Alkenyl; Acyl; Fluxionality; Diphosphine; Phosphide

1. Introduction

We have recently been concerned with the synthesis and reactivity of hydrido–diiron complexes in which the integrity of the diiron centre is maintained by the presence of a bridging diphosphine ligand [1–5]. Examples include the phosphido-bridged complexes [$Fe_2(CO)_4(\mu$-H)(μ-CO)(μ-PR_2)(μ-dppm)] **1a–b** (R = Ph, Cy) which have been shown to undergo hydrodimetalation reactions towards a range of unsaturated organic molecules [1,3,4]. Thus, primary alkynes react readily at room temperature, resulting in CO loss and giving rise to σ–π alkenyl complexes [2,5]. Even in this relatively simple insertion reaction a number of isomeric products is possible. Based on the regioselectivity of the hydrodimetalation process, α- and β-substituted alkenyls can form, while further isomers result from the relative orientation of the diphosphine and phosphido ligands (*cis* or *trans*). The latter stems from the different relative orientations of these ligands in **1a** and **1b**; ^{31}P NMR data for the former being strongly suggestive of a relative *cis* orientation [2], while X-ray diffraction studies of the latter revealed a *trans* arrangement [5]. This seemingly simple difference between **1a** and **1b** can lead to quite different reaction products. Thus, in all reactions of **1b** studied to date the *trans* arrangement of diphosphine and phosphido ligands is maintained. In contrast, during hydrodimetalation reactions involving **1a** products are found in which the initial *cis* arrangement of diphosphine and phosphido ligands is maintained, while others result from a *cis–trans* rearrange-

* Corresponding author. E-mail: uccaxgh@ucl.ac.uk.

0022-328X/97/$17.00 © 1997 Elsevier Science S.A. All rights reserved.
PII S0022-328X(96)06643-0

ment of these ligands. [It should be noted that while in theory four arrangements of the three bridging ligands are possible, in practice since the three-electron donor phosphido and organic ligands are constrained to lie *cis* to one another, only two possible arrangements of the three ligands are found.]

The insertion of phenylethyne into **1a–b** serves to illustrate these points. We have previously found that reaction with **1a** affords a chromatographically inseparable mixture of two isomers [2]. The major isomer (10:1) was readily identified on the basis of NMR studies as *cis*-[$Fe_2(CO)_4(\mu$-PhC=$CH_2)(\mu$-$PPh_2)(\mu$-dppm)] **2a**, and results from a Markovnikov addition (that is to give the α-substituted alkenyl) with retention of the phosphine bridge arrangement. The nature of the minor isomer, however, was more contentious. Phosphorus-31 NMR data were clearly indicative of a *trans* arrangement of diphosphine and phosphido bridges, however, in the ^{1}H NMR spectrum resonances associated with this isomer were not clearly resolved, being partially obscured by those of the major isomer **2a**. Thus, primarily on the basis of favouring a Markovnikov insertion process, we initially (but erroneously) assigned the minor isomer as *trans*-[$Fe_2(CO)_4(\mu$-PhC=$CH_2)(\mu$-$PPh_2)(\mu$-dppm)] **2c** [2]. Reaction of phenylethyne with **1b** at first sight appears to be straightforward, since after chromatography only the β-substituted complex *trans*-[$Fe_2(CO)_4(\mu$-HC=CHPh)$(\mu$-$PCy_2)(\mu$-dppm)] **3a** was isolated, albeit in moderate yield [5]. Unambiguous characterisation was based on both solution NMR data and a single crystal X-ray diffraction study. We were, however, concerned at the low yields and wondered if other products had been formed, most notably the α-substituted isomer, that did not survive the work-up procedures.

The reactions detailed above serve to underline some major differences in the chemistry of seemingly similar *cis*-[$Fe_2(CO)_4(\mu$-H)$(\mu$-CO)$(\mu$-$PPh_2)(\mu$-dppm)] **1a** and *trans*-[$Fe_2(CO)_4(\mu$-H)$(\mu$-CO)$(\mu$-$PCy_2)(\mu$-dppm)] **1b**. Thus, while in **1a** there is a strong preference for Markovnikov hydrodimetalation, in contrast with **1b** anti-Markovnikov addition dominates. Further, while with phenylethyne the initial arrangement of phosphorus-containing ligands is maintained throughout both reactions, this is not always so. For example, reaction of either **1a** or **1b** with ethyne affords *trans*-[$Fe_2(CO)_4(\mu$-HC=$CH_2)(\mu$-$PR_2)(\mu$-dppm)] (R = Ph, Cy) as the only reaction products in high yield [2,5]. Thus, while the *trans* arrangement of phosphorus-containing ligands is fixed in **1b**, for **1a** their relative mobility is strongly dependent upon the nature of the reactant. Clearly, in order to be absolutely certain as to the nature of the alkenyl complexes produced, single crystal X-ray diffraction results are of paramount importance. In this paper we give details of the crystal structures of three μ-alkenyl complexes, including those of both isomers of the phenylethyne insertion into **1a**, together with the structure of an α,β-unsaturated acyl complex which we believe is formed as a result of 'trapping-out' the putative second isomer of the phenylethyne insertion into **1b**.

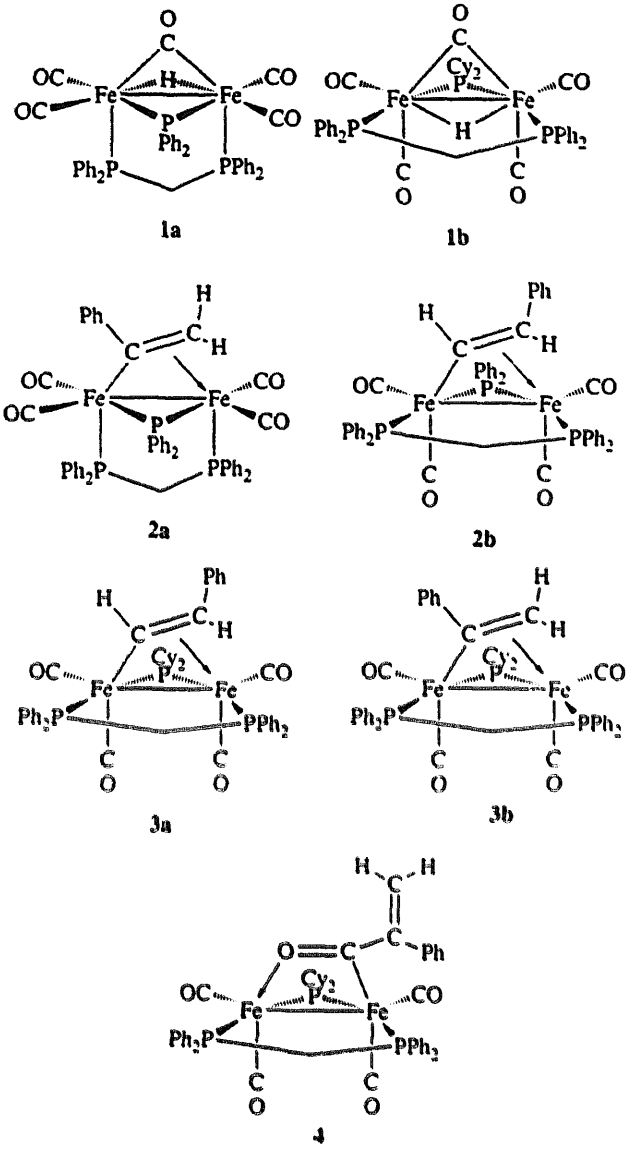

2. Experimental details

2.1. General comments

All reactions were carried out under N_2 in predried solvents. NMR spectra were recorded on a Varian VXR 400 spectrometer and IR spectra on a Nicolet 205 Fourier transform spectrometer. Chromatography was carried out on columns of deactivated alumina (6%

w/w water). Elemental analyses were performed in the Chemistry Department of University College. Propargyl alcohol was purchased from Aldrich and used without further purification. The complexes $[Fe_2(CO)_4(\mu\text{-}H)(\mu\text{-}CO)(\mu\text{-}PR_2)(\mu\text{-dppm})]$ **1a–b** [2,5] and mixtures of *cis*-$[Fe_2(CO)_4(\mu\text{-}PhC{=}CH_2)(\mu\text{-}PPh_2)(\mu\text{-dppm})]$ **2a** and *trans*-$[Fe_2(CO)_4(\mu\text{-}HC{=}CHPh)(\mu\text{-}PPh_2)(\mu\text{-dppm})]$ **2b** [2] were prepared as previously described.

2.2. Separation of *cis*-$[Fe_2(CO)_4(\mu\text{-}PhC{=}CH_2)(\mu\text{-}PPh_2)(\mu\text{-dppm})]$ 2a and *trans*-$[Fe_2(CO)_4(\mu\text{-}HC{=}CHPh)(\mu\text{-}PPh_2)(\mu\text{-dppm})]$ 2b

Thermolysis of a toluene solution (50 cm^3) of a mixture of **2a** and **2b** (10:1) resulted in a colour change from orange to red. Removal of volatiles gave an oily red solid which was chromatographed on alumina. Two as yet unidentified bands eluted with light petroleum and diethylether (10:1, yellow; 5:1, orange). Further elution with light petroleum and diethylether (4:1) gave a yellow band which afforded **2b** (0.04 g) as a yellow solid. Slow diffusion of methanol into a concentrated dichloromethane solution gave large yellow crystals. Orange crystals of **2a** were formed in an analogous fashion from the initial mixture. **2a**: IR (CH_2Cl_2) ν(CO) 1974 m, 1947 s, 1907 m cm^{-1}; ^{13}C NMR ($CDCl_3$, 293 K) 219.6 (br, 4CO), 190.5 (br, C_α), 140–124 (m, Ph), 59.95 (d, J 11.8, C_β), 41.84 (t, J 20.2, CH_2) ppm. **2b**: IR (CH_2Cl_2) ν(CO) 1980 m, 1947 s, 1917, 1901 sh cm^{-1}; ^1H NMR ($CDCl_3$, 293 K) δ 7.80–6.20 (m, 35H, Ph), 6.95 (m, 1H, CH), 4.79 (ddd, J 14.0, 4.8, 2.0, 1H, CHPh), 3.88 (m, 1H, CH_2), 2.73 (dt, J 14.4, 10.1, 1H, CH_2); ^{13}C NMR ($CDCl_3$, 293 K) 219.17 (br, 2CO), 219.10 (m, 2CO), 143.8 (m, C_α), 142–124 (Ph), 99.63 (d, J 23.1, C_β), 40.40 (t, J 19.7, CH_2) ppm; mass spectrum (FAB) m/e 896, 868, 840, 812, 784; Anal. Found: C, 60.77; H, 4.32. $Fe_2C_{49}H_{39}O_4P_3 \cdot CH_2Cl_2$ Calc.: C, 61.16; H, 4.18%.

2.3. Synthesis of *trans*-$[Fe_2(CO)_4\{\mu\text{-}O{=}C\text{-}C(Ph){=}CH_2\}(\mu\text{-}PCy_2)(\mu\text{-dppm})]$ 4

The reaction of **1b** (0.40 g, 0.48 mmol) with phenylethyne was carried out as previously described [5], however, prior to chromatography the toluene solution was refluxed for 3 h. Following this, chromatography was carried out. Elution with light petroleum and diethylether (20:1) gave a yellow–orange band which afforded **4** (0.01 g, 3%) as an orange solid. Slow diffusion of methanol into a dichloromethane solution gave orange crystals suitable for X-ray diffraction. Elution with light petroleum and diethylether (10:1) gave an orange band of **3a** [5]. **4**: IR (CH_2Cl_2) ν(CO) 1972 mm, 1942 s, 1905 m, 1890 sh, 1606 m (C=C), 1450 w (C=O acyl) cm^{-1}; ^1H NMR ($CDCl_3$, 293 K) δ 7.8–6.8 (m, 25H, Ph), 3.50 (br, 2H, $C{=}CH_2$), 3.06 (br, 1H, CH_2), 2.50 (br, 1H, CH_2), 2.1–0.8 (m, 22H, Cy); ^{31}P NMR ($CDCl_3$, 293 K) 258.2 (dd, J 103, 56, μ-PCy_2), 59.4 (dd, J 63, 56, PPh_2), 46.7 (dd, J 103, 63, PPh_2) ppm; mass spectrum (FAB) m/e 937, 909, 881, 852, 824, 796.

2.4. Synthesis of *cis*-$[Fe_2(CO)_4\{\mu\text{-}C(CH_2OH){=}CH_2\}(\mu\text{-}PPh_2)(\mu\text{-dppm})]$ 5a and *trans*-$[Fe_2(CO)_4\{\mu\text{-}HC{=}CH(CH_2OH)\}(\mu\text{-}PPh_2)(\mu\text{-dppm})]$ 5b

Addition of propargyl alcohol (0.1 cm^3, 1.70 mmol) to a toluene solution of **1a** (0.40 g, 0.49 mmol) and stirring at room temperature for 12 h resulted in the formation of a reddish brown solution which, on removal of volatiles and washing with light petroleum, afforded an orange solid. Chromatography, eluting with light petroleum and dichloromethane (3:2) gave a yellow band which afforded **5b** (0.13 g, 31%). Further elution with light petroleum and dichloromethane (2:3) gave a yellow band which afforded **5a** (0.10 g, 23%) as a yellow solid. Slow diffusion of methanol into a dichloromethane solution gave orange crystals suitable for X-ray diffraction. **5a**: IR (CH_2Cl_2) ν(CO) 1982 m, 1959 s, 1921 m, 1900 sh cm^{-1}; ^1H NMR ($CDCl_3$, 293 K) δ 7.8–6.8 (m, 30H, Ph), 3.75 (1H, m, CH_2), 3.40 (m, 1H, CH_2), 3.00 (d, J 7.2, 2H, CH_2O), 2.20 (1H, br, $C{=}CH_2$, 2.00 (1H, br, $C{=}CH_2$); ^{31}P NMR (toluene-d_8, 253 K) 174.3 (dd, J 47, 24, μ-PPh_2), 62.8 (dd, J 95, 24, PPh_2), 42.8 (dd, J 95, 47, PPh_2) ppm; Anal. Found: C, 60.95; H, 4.73; P, 10.71. $Fe_2C_{44}H_{37}O_5P_3$ Calc.: C, 61.25; H, 4.68; P, 10.53%. **5b**: IR (CH_2Cl_2) ν(CO) 1982 m, 1951 s, 1919 m cm^{-1}; ^1H NMR ($CDCl_3$, 293 K) δ 7.9–7.1 (m, 30H, Ph), 6.50 (m, 1H, H_α), 3.75 (m, 1H, CH_2), 3.50 (br, 1H, H_β), 2.76 (m, 1H, CH_2), 2.20 (br, 2H, CH_2O); ^{31}P NMR (toluene-d_8, 253 K) 207.6 (t, J 83, μ-PPh_2), 84.3 (t, J 73, PPh_2), 78.8 (t, 81, PPh_2) ppm.

2.5. Synthesis of *trans*-$[Fe_2(CO)_4\{\mu\text{-}C(CH_2OH){=}CH_2\}(\mu\text{-}PCy_2)(\mu\text{-dppm})]$ 6a and *trans*-$[Fe_2(CO)_4\{\mu\text{-}HC{=}CH(CH_2OH)\}(\mu\text{-}PCy_2)(\mu\text{-dppm})]$ 6b

Addition of propargyl alcohol (0.1 cm^3, 1.70 mmol) to a toluene solution of **1b** (0.40 g, 0.48 mmol) resulted, after stirring at room temperature for 12 h, in the formation of a red solution which afforded an orange solid upon removal of volatiles. Chromatography, eluting with light petroleum and dichloromethane (9:1) gave a yellow band which afforded a mixture of **6a** and **6b** (0.27 g, 66%) as a yellow solid. **6**: IR (CH_2Cl_2) ν(CO) 1970 m, 1942 s, 1910 m, 1901 sh cm^{-1}; Anal. Found: C, 61.34; H, 4.98. $Fe_2C_{44}H_{50}O_5P_3$ Calc.: C, 61.18; H, 5.10%. **6a**: ^1H NMR ($CDCl_3$, 293 K) δ 8.2–7.0 (m, 20H, Ph), 6.28 (m, 1H, H_α), 4.03 (br, 1H, H_β), 3.81 (q,

J 11.0, 1H, CH_2), 2.71 (dt, J 14.3, 9.5, 1H, CH_2), 2.40 (br, 2H, CH_2O), 2.1–1.0 (m, 22H, Cy); ^{31}P NMR ($CDCl_3$, 253 K) 242.9 (t, J 79, μ-PCy_2), 82.4 (t, J 70, PPh_2), 79.1 (t, J 83, PPh_2) ppm. **6b**: ^1H NMR ($CDCl_3$, 293 K) δ 3.6 (m, 2H, CH_2), 2.98 (d, J 8.1, 2H, C=CH_2) (other signals obscured); ^{31}P NMR ($CDCl_3$, 253 K) 246.2 (t, J 77, μ-PCy_2), 76.5 (m, second order, 2PPh_2) ppm.

2.6. X-ray data collection and solution

For all structures, a single crystal was mounted on a glass fibre and all geometric and intensity data were taken from this sample using an automated four-circle diffractometer (Nicolet R3mV) equipped with Mo Kα radiation (λ = 0.71073 Å). Important crystallographic parameters are summarised in Table 1. The lattice vectors were identified by application of the automatic indexing routine of the diffractometer to the positions of a number of reflections taken from a rotation photograph and centred by the diffractometer. The ω–2θ (**2b** and **5a**) or ω (**2a** and **4**) techniques were used to measure reflections in the range $5° \leq 2\theta \leq 50°$ (**2a–b**, **5a**) or $5° \leq 2\theta \leq 42°$ (**4**). Three standard reflections (remeasured every 97 scans) showed no significant loss in intensity during data collection. The data were corrected for Lorentz and polarisation effects, and empirically for absorption except in the case of **4**. The unique data with $I \geq 3.0\sigma(I)$ were used to solve and refine the structures.

Structures were solved by direct methods and developed by using alternating cycles of least-squares refinement and difference Fourier synthesis. All non-hydrogen atoms were refined anisotropically for **2a–b**, while for **5a** phenyl rings were refined isotropically and for **4** only the iron and phosphorus atoms were refined anisotropically. Hydrogens were placed in idealised positions (C–H 0.96 Å) and assigned a common isotropic thermal parameter ($U = 0.08$ Å^2). The non-hydrogen atoms of the dichloromethane were refined only isotropically in **2b**. Final difference Fourier maps were featureless and contained no peaks greater than 1.00 e Å^{-3}, except in **2b** which showed a number of larger peaks close to the dichloromethane solvate. Structure solution used the SHELXTL-PLUS program package on a microVax II computer [6].

Tables 2–5 give atomic coordinates and equivalent isotropic displacement parameters for **2a**, **2b**, **4** and **5a** respectively. A complete list of bond lengths and angles

Table 1
Crystallographic data

	2a · CH_2Cl_2	**2b** · CH_2Cl_2	**4**	**5a**
Formula	$Fe_2C_{50}H_{41}O_4P_3Cl_2$	$Fe_2C_{50}H_{41}O_4P_3Cl_2$	$Fe_2C_{50}H_{51}O_3P_3$	$Fe_2C_{45}H_{37}O_3P_3$
Space group	$P2_1/n$	$P\bar{1}$	$P2_1/c$	$P2_1/c$
a (Å)	11.830(4)	12.397(4)	16.443(5)	16.693(3)
b (Å)	27.889(8)	12.438(5)	11.606(3)	18.019(8)
c (Å)	14.506(5)	18.298(6)	24.388(6)	20.353(9)
α (deg)	90	104.06(3)	90	90
β (deg)	105.14(3)	92.09(3)	100.60(2)	93.83(3)
γ (deg)	90	119.59(2)	90	90
V (Å^3)	4619.7	2338.6	4574.5	3912.7
Z	4	2	4	4
F(000)	1976	1008	1952	1776
d_{calc} (g cm^{-3})	1.40	1.39	1.36	1.46
Crystal size (mm^3)	0.62 × 0.42 × 0.27	0.76 × 0.46 × 0.24	0.26 × 0.20 × 0.12	0.36 × 0.30 × 0.24
μ(Mo Kα) (cm^{-1})	8.89	8.78	7.81	9.07
Orientation reflections: no.; range	20; $15° \leq 2\theta \leq 28°$	27; $18° \leq 2\theta \leq 28°$	21; $10° \leq 2\theta \leq 18°$	28; $10° \leq 2\theta \leq 20°$
Data measured	9354	8978	5629	7584
Unique data	8976	8277	5194	7239
No. of unique data with $I \geq 3.0\sigma(I)$	6638	6129	2241	3175
No. of parameters	550	535	266	307
R [a]	0.051	0.059	0.069	0.062
R_w [b]	0.057	0.067	0.069	0.063
Weighting scheme	$W^{-1} = \sigma^2(F) + 0.001015F^2$	$W^{-1} = \sigma^2(F) + 0.000889F^2$	$W^{-1} = \sigma^2(F) + 0.000505F^2$	$W^{-1} = \sigma^2(F) + 0.000696F^2$
Largest shift/e.s.d., final cycle	0.10	0.001	0.05	0.05
Largest peak (e Å^{-3})	0.80	1.51	0.45	0.72

[a] $R = \Sigma[|F_o| - |F_c|]/\Sigma|F_o|$.
[b] $R_w = \Sigma w^{1/2}[|F_o| - |F_c|]/\Sigma w^{1/2}|F_o|$.

Table 2
Atomic coordinates ($\times 10^4$) and equivalent isotropic displacement parameters (Å$\times 10^3$) for **2a**

Atom	x	y	z	U_{eq} *
Fe(1)	3361(1)	1081(1)	1533(1)	29(1)
Fe(2)	2494(1)	1918(1)	809(1)	32(1)
P(1)	4396(1)	1297(1)	3015(1)	32(1)
P(2)	3813(1)	2260(1)	2022(1)	33(1)
P(3)	1731(1)	1409(1)	1721(1)	31(1)
O(1)	5586(3)	803(1)	1153(3)	57(1)
O(2)	2741(4)	84(1)	1677(3)	66(2)
O(3)	3381(4)	2518(1)	−488(3)	67(2)
O(4)	384(3)	2495(2)	544(3)	75(2)
C(1)	4717(4)	935(2)	1289(3)	39(2)
C(2)	2989(4)	484(2)	1646(3)	39(2)
C(3)	3080(4)	2263(2)	28(3)	44(2)
C(4)	1233(4)	2277(2)	660(3)	45(2)
C(5)	2739(4)	1241(1)	159(3)	35(1)
C(6)	1644(4)	1447(2)	−306(3)	42(2)
C(7)	4242(4)	1948(1)	3181(3)	34(1)
C(10)	4118(4)	1042(2)	4105(3)	38(1)
C(11)	3735(5)	574(2)	4104(4)	52(2)
C(12)	3585(6)	367(2)	4918(4)	67(2)
C(13)	3802(6)	631(2)	5769(4)	71(3)
C(14)	4183(6)	1090(2)	5769(4)	71(2)
C(15)	4367(5)	1298(2)	4955(4)	57(2)
C(20)	5975(4)	1176(2)	3312(3)	36(1)
C(21)	6303(4)	695(2)	3385(4)	48(2)
C(22)	7470(5)	567(2)	3596(4)	61(2)
C(23)	8306(5)	910(2)	3736(5)	64(2)
C(24)	8005(5)	1387(2)	3660(5)	64(2)
C(25)	6839(4)	1521(2)	3452(4)	47(2)
C(30)	3391(4)	2858(2)	2364(4)	45(2)
C(31)	2960(6)	3187(2)	1639(5)	67(2)
C(32)	2649(7)	3643(2)	1858(6)	89(3)
C(33)	2774(6)	3773(2)	2797(6)	81(3)
C(34)	3181(6)	3459(2)	3491(6)	75(3)
C(35)	3498(5)	2998(2)	3293(4)	58(2)
C(40)	5271(4)	2390(2)	1838(3)	39(1)
C(41)	5742(4)	2093(2)	1274(4)	47(2)
C(42)	6885(5)	2173(2)	1197(4)	63(2)
C(43)	7531(5)	2544(3)	1675(5)	70(2)
C(44)	7069(5)	2841(3)	2239(5)	72(2)
C(45)	5941(5)	2770(2)	2312(4)	56(2)
C(50)	313(4)	1112(2)	1232(3)	37(1)
C(51)	−692(4)	1268(2)	1472(4)	47(2)
C(52)	−1747(4)	1039(2)	1135(4)	56(2)
C(53)	−1854(4)	657(2)	511(5)	58(2)
C(54)	−871(4)	500(2)	250(5)	61(2)
C(55)	202(4)	720(2)	613(4)	48(2)
C(60)	1480(4)	1613(2)	2851(3)	39(2)
C(61)	1402(4)	1273(2)	3526(3)	49(2)
C(62)	1173(5)	1410(2)	4380(4)	62(2)
C(63)	989(5)	1888(3)	4535(4)	70(3)
C(64)	1054(5)	2228(2)	3874(5)	69(2)
C(65)	1303(4)	2093(2)	3036(4)	52(2)
C(70)	3468(4)	1097(2)	−497(3)	41(2)
C(71)	3374(6)	625(2)	−787(4)	68(3)
C(72)	4080(7)	442(3)	−1343(5)	84(3)
C(73)	4837(7)	732(3)	−1642(5)	80(3)
C(74)	4927(6)	1203(3)	−1379(4)	76(3)
C(75)	4231(5)	1385(2)	−827(4)	59(2)
C(100)	10401(14)	414(7)	7610(10)	263(12)
Cl(1)	9375(6)	114(2)	6598(8)	375(7)
Cl(2)	11019(6)	814(2)	6872(5)	273(4)

* Equivalent isotropic U defined as one third of the trace of the orthogonalized U_{ij} tensor.

Table 3
Atomic coordinates ($\times 10^4$) and equivalent isotropic displacement parameters (Å$\times 10^3$) for **2b**

Atom	x	y	z	U_{eq} *
Fe(1)	3446(1)	9065(1)	2132(1)	28(1)
Fe(2)	1926(1)	9736(1)	2685(1)	27(1)
P(1)	2272(1)	6968(1)	2028(1)	28(1)
P(2)	464(1)	7801(1)	2769(1)	27(1)
P(3)	3693(1)	10982(1)	2294(1)	31(1)
O(1)	2898(6)	8430(5)	463(3)	72(3)
O(2)	5990(5)	9545(5)	2244(3)	72(3)
O(3)	586(5)	8970(4)	1139(2)	54(2)
O(4)	1131(6)	11509(4)	3429(3)	61(3)
C(1)	3121(6)	8685(5)	1124(3)	43(3)
C(2)	4976(6)	9342(5)	2218(3)	41(3)
C(3)	1128(6)	9266(5)	1751(3)	37(3)
C(4)	1447(6)	10793(5)	3150(3)	38(3)
C(5)	3162(5)	9317(5)	3201(3)	31(2)
C(6)	3359(5)	10413(5)	3764(3)	33(2)
C(7)	641(5)	6535(5)	2129(3)	30(2)
C(10)	2046(5)	5812(5)	1110(3)	31(2)
C(11)	3121(6)	5999(6)	818(3)	43(3)
C(12)	3017(7)	5140(6)	133(4)	54(4)
C(13)	1857(7)	4099(6)	−258(3)	51(4)
C(14)	792(7)	3918(6)	33(3)	52(3)
C(15)	882(6)	4774(6)	702(3)	45(3)
C(20)	2663(5)	6272(5)	2699(3)	33(3)
C(21)	3661(6)	7023(6)	3296(3)	43(3)
C(22)	3864(7)	6495(7)	3850(4)	60(4)
C(23)	3046(8)	5200(8)	3768(5)	68(5)
C(24)	2067(7)	4425(6)	3151(4)	55(4)
C(25)	1870(6)	4963(6)	2619(4)	46(3)
C(30)	371(5)	7504(5)	3706(3)	30(2)
C(31)	609(6)	6618(5)	3889(3)	42(3)
C(32)	535(7)	6461(7)	4605(4)	56(4)
C(33)	197(7)	7183(8)	5155(4)	62(4)
C(34)	−42(6)	8066(7)	4966(3)	51(3)
C(35)	62(5)	8229(6)	4252(3)	41(3)
C(40)	−1204(5)	7187(5)	2430(3)	35(3)
C(41)	−1591(6)	7983(6)	2265(3)	45(3)
C(42)	−2862(6)	7488(7)	1983(4)	54(4)
C(43)	−3734(7)	6204(8)	1878(4)	63(4)
C(44)	−3352(7)	5397(8)	2029(4)	62(4)
C(45)	−2119(6)	5886(6)	2315(4)	49(3)
C(50)	3636(5)	11545(5)	1462(3)	39(3)
C(51)	2823(7)	11953(7)	1340(5)	64(4)
C(52)	2820(11)	12406(11)	741(7)	104(6)
C(53)	3602(10)	12440(9)	233(5)	86(6)
C(54)	4410(9)	12037(8)	338(5)	73(5)
C(55)	4444(7)	11591(6)	969(4)	54(3)
C(60)	4985(6)	12491(5)	2958(3)	39(3)
C(61)	6143(6)	12632(6)	3176(4)	57(3)
C(62)	7101(8)	13767(8)	3680(5)	76(4)
C(63)	6910(8)	14796(8)	3994(5)	78(4)
C(64)	5793(8)	14644(7)	3783(5)	76(4)
C(65)	4833(7)	13517(6)	3275(4)	58(3)
C(70)	3138(5)	10447(5)	4562(3)	33(2)
C(71)	3309(6)	9670(6)	4927(3)	41(3)
C(72)	3190(7)	9781(7)	5684(4)	55(4)
C(73)	2897(7)	10656(7)	6091(4)	60(4)
C(74)	2735(6)	11439(7)	5739(4)	53(3)
C(75)	2874(6)	11354(6)	4980(3)	45(3)
C(100)	8174(14)	1276(13)	1131(8)	130(4)
C1(1)	8094(4)	2528(4)	1614(3)	158(1)
C1(2)	9340(8)	1109(7)	1514(4)	246(3)

* Equivalent isotropic U defined as one third of the trace of the orthogonalized U_{ij} tensor.

Table 4
Atomic coordinates ($\times 10^4$) and equivalent isotropic displacement parameters (Å$\times 10^3$) for **4**

Atom	x	y	z	U_{eq} *
Fe(1)	3205(1)	1358(2)	9484(1)	36(1)
Fe(2)	2288(1)	2458(2)	8645(1)	37(1)
P(1)	2753(3)	2207(3)	10204(2)	39(2)
P(2)	1813(2)	3614(3)	9246(2)	38(2)
P(3)	3205(3)	1065(4)	8583(2)	44(2)
O(1)	4658(6)	2790(9)	9527(4)	52(3)
O(2)	4178(7)	−532(10)	10039(5)	67(3)
O(3)	3378(8)	4205(11)	8287(5)	82(4)
O(4)	1263(8)	2580(12)	7556(6)	98(4)
O(5)	2091(5)	626(7)	9328(3)	32(3)
C(1)	4057(9)	2242(12)	9517(6)	41(4)
C(2)	3746(10)	213(15)	9832(7)	57(5)
C(3)	2946(10)	3513(15)	8445(7)	59(5)
C(4)	1634(11)	2550(15)	8000(7)	65(5)
C(5)	1679(9)	1231(13)	8933(6)	46(4)
C(6)	780(9)	883(13)	8775(6)	42(4)
C(7)	226(10)	1555(15)	8474(6)	64(5)
C(8)	1750(8)	2937(12)	9936(5)	35(4)
C(10)	2484(9)	1224(13)	10738(6)	45(4)
C(11)	2491(10)	1586(16)	11276(7)	72(6)
C(12)	2308(11)	786(17)	11681(9)	85(6)
C(13)	2083(11)	−271(15)	11540(7)	66(5)
C(14)	2085(10)	−680(16)	11005(7)	74(6)
C(15)	2275(10)	99(14)	10602(7)	57(5)
C(20)	3377(9)	3295(13)	10638(6)	46(4)
C(21)	3062(11)	4253(14)	10842(7)	59(5)
C(22)	3578(12)	5070(17)	11169(7)	82(6)
C(23)	4393(13)	4870(17)	11267(8)	84(6)
C(24)	4731(12)	3931(15)	11084(7)	72(6)
C(25)	4237(10)	3117(15)	10764(6)	58(5)
C(30)	2373(9)	4959(13)	9485(6)	38(4)
C(31)	1928(11)	5902(14)	9623(6)	58(5)
C(32)	2390(11)	6886(15)	9861(7)	64(5)
C(33)	3227(10)	6881(15)	9945(7)	65(5)
C(34)	3657(11)	5956(13)	9790(6)	57(5)
C(35)	3216(9)	4975(13)	9551(6)	45(4)
C(40)	750(9)	4159(12)	9015(6)	40(4)
C(41)	134(9)	3981(12)	9313(6)	45(4)
C(42)	−678(11)	4355(14)	9089(7)	61(5)
C(43)	−816(12)	4886(15)	8592(7)	71(6)
C(44)	−227(11)	5076(15)	8292(7)	69(5)
C(45)	584(11)	4707(14)	8498(7)	59(5)
C(50)	2929(9)	−394(13)	8272(6)	48(5)
C(51)	3042(11)	−1350(15)	8680(7)	73(6)
C(52)	2881(11)	−2506(16)	8393(7)	82(6)
C(53)	2080(12)	−2602(17)	8011(8)	94(7)
C(54)	1941(12)	−1636(15)	7595(8)	88(6)
C(55)	2108(11)	−450(16)	7877(8)	81(6)
C(60)	4152(9)	1451(14)	8317(6)	48(4)
C(61)	4845(11)	606(15)	8501(7)	75(6)
C(62)	5639(13)	1024(20)	8330(9)	114(8)
C(63)	5516(14)	1343(20)	7728(9)	121(8)
C(64)	4818(12)	2116(17)	7528(8)	96(7)
C(65)	4000(10)	1631(15)	7671(7)	69(5)
C(70)	501(9)	−225(12)	8960(6)	37(4)
C(71)	594(10)	−521(14)	9526(7)	56(5)
C(72)	313(10)	−1606(14)	9671(7)	63(5)
C(73)	−39(10)	−2354(16)	9291(7)	67(5)
C(74)	−147(10)	−2080(14)	8736(7)	60(5)
C(75)	128(10)	−1022(14)	8578(7)	62(5)

* Equivalent isotropic U defined as one third of the trace of the orthogonalized U_{ij} tensor.

Table 5
Atomic coordinates ($\times 10^4$) and equivalent isotropic displacement parameters (Å$\times 10^3$) for **5a**

Atom	x	y	z	U_{eq} *
Fe(1)	2569(1)	7740(1)	1789(1)	36(1)
Fe(2)	4562(1)	6863(1)	1934(1)	37(1)
P(1)	2766(2)	8227(1)	769(1)	35(1)
P(2)	5317(2)	7504(1)	1100(1)	34(1)
P(3)	2688(2)	6573(1)	1398(1)	33(1)
O(1)	2836(8)	9256(5)	2315(4)	74(4)
O(2)	−89(8)	7838(5)	2019(5)	86(4)
O(3)	5397(9)	5334(5)	1768(4)	78(4)
O(4)	6760(8)	7282(6)	2789(4)	88(4)
O(5)	4482(11)	7525(6)	3725(4)	109(5)
C(1)	2808(11)	8655(7)	2104(5)	54(4)
C(2)	951(12)	7802(7)	1909(5)	59(5)
C(3)	5113(10)	5957(7)	1823(5)	49(4)
C(4)	5890(12)	7148(7)	2446(5)	61(5)
C(5)	3380(9)	7310(6)	2629(4)	46(4)
C(6)	3548(9)	6555(6)	2772(4)	45(4)
C(7)	3825(11)	7868(7)	3183(5)	62(5)
C(8)	4200(8)	7853(5)	431(4)	35(3)
C(11)	2879(9)	9249(5)	742(5)	42(3)
C(12)	3959(10)	9636(6)	711(5)	49(3)
C(13)	3973(12)	10420(7)	779(6)	64(3)
C(14)	2889(12)	10789(8)	881(6)	73(4)
C(15)	1783(13)	10412(8)	909(6)	78(4)
C(16)	1764(11)	9643(7)	840(5)	60(3)
C(21)	1597(9)	8082(5)	77(4)	37(2)
C(22)	1909(10)	8145(6)	−571(5)	50(3)
C(23)	1026(10)	8016(6)	−1100(6)	58(3)
C(24)	−177(10)	7828(6)	−972(6)	58(3)
C(25)	−528(10)	7789(6)	−338(5)	51(3)
C(26)	336(9)	7906(5)	186(5)	43(3)
C(31)	6222(9)	8355(5)	1289(5)	38(2)
C(32)	5972(10)	8793(6)	1835(5)	47(3)
C(33)	6537(10)	9492(7)	1929(6)	59(3)
C(34)	7376(11)	9735(7)	1488(6)	65(3)
C(35)	7645(11)	9315(5)	952(6)	62(3)
C(36)	7055(10)	8630(6)	862(5)	51(3)
C(41)	6451(8)	6972(5)	631(4)	33(2)
C(42)	6279(9)	6849(6)	−36(5)	44(3)
C(43)	7094(10)	6365(6)	−344(5)	50(3)
C(44)	8050(10)	6011(6)	8(5)	55(3)
C(45)	8232(10)	6151(6)	672(5)	51(3)
C(46)	7432(9)	6628(6)	986(5)	45(3)
C(51)	1677(9)	5824(5)	1697(5)	38(2)
C(52)	688(10)	5966(6)	2082(5)	50(3)
C(53)	−56(11)	5387(7)	2301(6)	61(3)
C(54)	212(12)	4667(7)	2137(6)	70(4)
C(55)	1197(11)	4507(7)	1771(6)	65(3)
C(56)	1939(10)	5084(6)	1553(5)	52(3)
C(61)	2638(8)	6255(5)	528(4)	34(2)
C(62)	3695(9)	5962(5)	261(4)	35(2)
C(63)	3626(10)	5698(6)	−380(5)	52(3)
C(64)	2531(9)	5713(5)	−762(5)	44(3)
C(65)	1470(11)	5988(6)	−496(5)	56(3)
C(66)	1512(9)	6257(5)	142(5)	39(2)

* Equivalent isotropic U defined as one third of the trace of the orthogonalized U_{ij} tensor.

and tables of hydrogen atom coordinates and anisotropic thermal parameters has been deposited at the Cambridge Crystallographic Data Centre.

3. Results and discussion

3.1. X-ray crystal structures of cis-[$Fe_2(CO)_4(\mu$-$PhC{=}CH_2)(\mu$-$PPh_2)(\mu$-dppm)] 2a and trans-[$Fe_2(CO)_4(\mu$-$HC{=}CHPh)(\mu$-$PPh_2)(\mu$-dppm)] 2b

As discussed in the Introduction, on the basis of spectroscopic studies in solution the precise nature of the minor isomer **2b** arising from the reaction of phenylethyne with *cis*-[$Fe_2(CO)_4(\mu$-H)(μ-PPh_2)(μ-dppm)] **1a** was not clear. In attempts to separate the two isomers, a mixture (10:1) was heated in toluene for 3 h during which time a number of changes were noted in the IR spectrum. After cooling to room temperature, chromatography revealed that the major isomer **2a** had been transformed into a number of as yet unknown products, while the minor isomer **2b** remained. Thus, we were able for the first time to obtain a pure sample of **2b**. In the carbonyl region of the IR spectrum absorptions at 1980 (m), 1947 (s), 1917 (m) and 1901 (sh) cm^{-1} for **2b** can be compared with those of **2a** [1974 (m), 1947 (s) and 1907 (m) cm^{-1}]. 31-Phosphorus NMR data were in accord with those reported previously [2], while in the ^1H NMR spectrum a slightly obscured low field multiplet at δ 6.95 was assigned to a proton bound to the α-carbon, indicating that it contained a β-substituted alkenyl ligand. In order to determine the precise nature of isomers **2a** and **2b**, single crystal X-ray diffraction studies were carried out on both, the results of which are given in Fig. 1 and Table 6.

Table 6
Selected bond lengths (Å) and angles (°) for **2a**, **2b** and **5a**

	2a	2b	5a
Fe(1)–Fe(2)	2.654(2)	2.561(2)	2.653(2)
Fe(1)–C(5)	1.998(9)	1.979(5)	2.019(9)
Fe(2)–C(5)	2.156(9)	2.106(7)	2.118(10)
Fe(1)–C(6)	3.074	3.426	3.062
Fe(2)–C(6)	2.141(9)	2.286(6)	2.154(10)
C(5)–C(6)	1.416(14)	1.397(8)	1.401(16)
Fe(1)–P(1)	2.257(3)	2.225(2)	2.276(3)
Fe(2)–P(2)	2.238(3)	2.234(2)	2.247(3)
Fe(1)–P(3)	2.214(3)	2.189(2)	2.256(3)
Fe(2)–P(3)	2.280(3)	2.239(2)	2.277(3)
Fe(1)–C(1)	1.778(5)	1.766(6)	1.780(12)
Fe(1)–C(2)	1.742(5)	1.745(8)	1.767(13)
Fe(2)–C(3)	1.760(5)	1.750(6)	1.756(12)
Fe(2)–C(4)	1.762(5)	1.752(8)	1.780(12)
Fe(1)–C(5)–Fe(2)	79.3(2)	77.6(2)	79.8(3)
Fe(1)–Fe(2)–C(6)	79.3(1)	78.8(2)	78.4(3)
Fe(2)–C(6)–C(5)	72.3(2)	64.6(3)	69.5(6)
Fe(1)–P(3)–Fe(2)	72.3(1)	70.6(1)	71.6(1)
P(1)–Fe(1)–C(5)	149.5(1)	84.1(2)	149.3(3)
P(2)–Fe(2)–C(5)	124.7(1)	82.6(1)	124.7(3)
P(3)–Fe(1)–C(5)	85.7(1)	84.5(2)	84.8(3)
P(3)–Fe(2)–C(5)	80.1(1)	80.4(2)	82.1(3)
P(1)–Fe(1)–P(3)	92.6(1)	151.9(1)	91.5(1)
P(2)–Fe(2)–P(3)	96.2(1)	150.5(1)	96.0(1)
C(1)–Fe(1)–Fe(2)	113.5(2)	108.0(3)	114.6(4)
C(2)–Fe(1)–Fe(2)	142.9(1)	147.3(2)	144.0(4)
C(3)–Fe(2)–Fe(1)	124.0(2)	89.0(3)	144.4(4)
C(4)–Fe(2)–Fe(1)	140.8(2)	157.0(2)	119.8(4)

The gross structural features of both complexes are as deduced from solution spectroscopic studies. Each contains a diiron tetracarbonyl core, bridged approximately symmetrically by phosphido and diphosphine ligands, with a third bridging site being occupied by the alkenyl ligand. The relative *cis* and *trans* arrangements of the phosphorus-containing ligands in **2a** and **2b** respectively are confirmed, as is the α-substituted na-

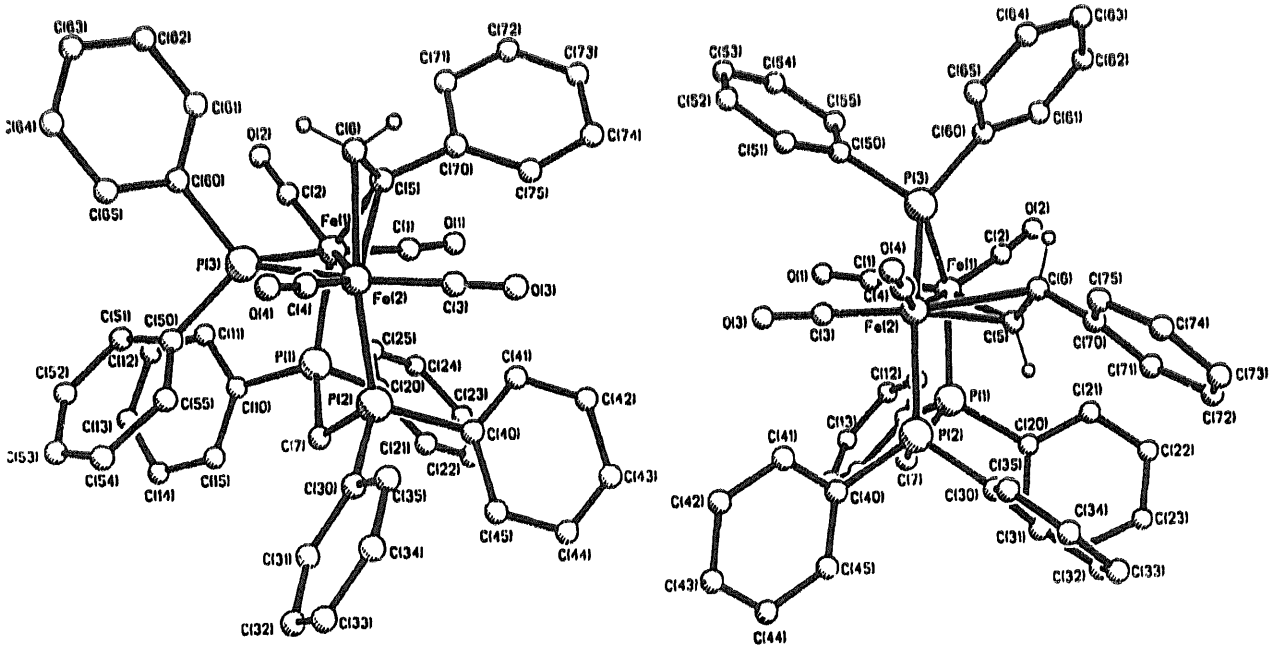

Fig. 1. Molecular structures of **2a** and **2b** respectively.

ture of the alkenyl ligand in the former. In **2b**, however, the phenyl ring is bound to the β-carbon of the alkenyl moiety, indicating that it arises as a result of an anti-Markovnikov insertion process.

As far as we are aware, this is the first time that isomeric α- and β-substituted μ-alkenyl complexes have been crystallographically characterised, and in light of this it is perhaps worthwhile taking a closer look at the solid state structures. Thus, while superficially similar, closer inspection reveals a number of significant and potentially important differences. Both are characterised by short iron–iron contacts indicative of a single metal–metal bond, however, that in **2a** [2.654(2) Å] is almost 0.1 Å longer than that in **2b** [2.561(2) Å]. Similarly, while in both complexes the iron–phosphorus bond lengths are within the expected ranges, it is noteworthy that in **2a** bonds to both phosphido and diphosphine ligands are slightly, but significantly, longer than those in **2b**. Perhaps the most important structural differences between the two can be found in the μ-alkenyl ligands themselves. Thus, while the Fe(1)–C_α bond lengths at 1.998(9) and 1.979(5) Å in **2a** and **2b** respectively are not significantly different, inspection of those to the second iron atom, Fe(2), reveal some rather dramatic differences. In **2a** it is bound almost symmetrically to both C_α and C_β [Fe(2)–C_α 2.156(9); Fe(2)–C_β 2.141(9) Å], the difference (Δ) being only 0.015 Å. In contrast, in **2b** the situation is radically different [Fe(2)–C_α 2.106(7); Fe(2)–C_β 2.286(6) Å], with a difference of some 0.180 Å, the shorter of the two being to C_α which contrasts with that found in **2a**. The C=C bond lengths of the alkenyl fragment do not appear to be affected by these differences, and values of 1.416(14) and 1.397(8) Å for **2a** and **2b** respectively do not differ significantly.

In light of the pronounced differences between the bonding of the μ-alkenyl ligands in **2a** and **2b**, it is worthwhile considering the well-known 'windshield-wiper' fluxionality in the two [4,7]. We have previously monitored this by variable temperature NMR spectroscopy and found large differences in the free energy of activation for the process, being calculated at 63 ± 1 and 45 ± 1 kJ mol^{-1} in **2a** (343K) and **2b** (223K) respectively. This difference manifests itself such that at room temperature the process is slow on the NMR timescale in **2a** but rapid in **2b**, only averaged signals being observed for the latter. We have previously been at a loss to account for this difference, but had tenta-

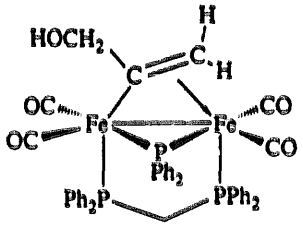

5a

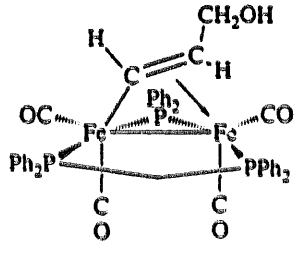

5b

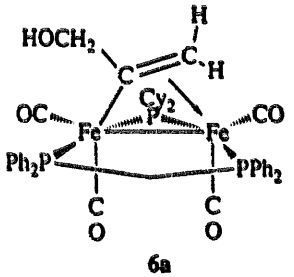

6a

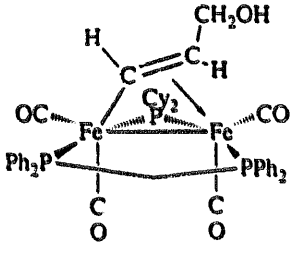

6b

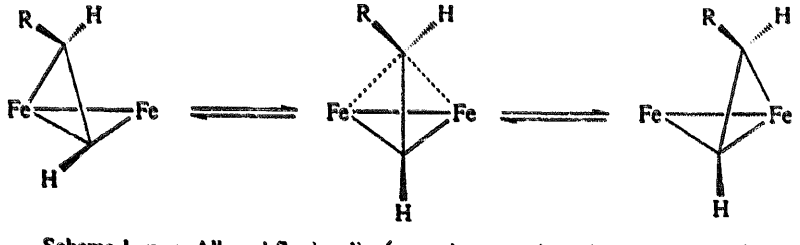

Scheme 1. σ–π Alkenyl fluxionality (assuming retention of stereochemistry).

tively attributed it to steric effects [2]. In light of the structural differences between **2a** and **2b**, a rethink is in order. The generally accepted mechanism for the 'windshield-wiper' process, based on a retention of stereochemistry, is shown in Scheme 1. Significantly, in the proposed transition state C_α and C_β are symmetrically bound to both metal centres, and it is the latter which moves to the greatest extent. Thus it might be expected that a complex in which, in the ground state, M–C_α bond lengths are similar and the M–C_β bond is elongated will have a low free energy of activation and thus be highly fluxional. Comparing **2a** and **2b**, it is clear that the latter fulfils these criteria, and thus it may be these ground state differences that lead to the large observed difference in the free energy of activation for the π-alkenyl 'windshield-wiper' fluxionality.

We also considered the possibility that the difference in free energy of activation for the alkenyl fluxionality in **2a–b** may be a consequence of the presence and relative orientation of the diphosphine ligand. Carty and coworkers [8] have reported the synthesis of the analogous hexacarbonyl complexes $[Fe_2(CO)_6(\mu\text{-}PhC{=}CH_2)(\mu\text{-}PPh_2)]$ and $[Fe_2(CO)_6(\mu\text{-}HC{=}CHPh)(\mu\text{-}PPh_2)]$, which can be separated by fractional crystallisation, and note that the energy barrier to the 'windshield-wiper' fluxionality is high. They did not, however, comment on any differences between the two isomers. In order to determine this we have reinvestigated these isomers by variable temperature ^{13}C NMR spectroscopy (the coalescence temperature of the carbonyl ligands was monitored) and find that they have very different free energies of activation, being calculated at $\geq 63 \pm 1$ and 52 ± 1 kJ mol^{-1} for α- and β-substituted isomers $[Fe_2(CO)_6(\mu\text{-}PhC{=}CH_2)(\mu\text{-}PPh_2)]$ ($\geq$ 350K) and $[Fe_2(CO)_6(\mu\text{-}HC{=}CHPh)(\mu\text{-}PPh_2)]$ (253K) respectively. These values are in accord with those found for **2a–b**, although the value for **2b** does appear to be significantly lower than those for other β-substituted complexes.

3.2. Synthesis and X-ray crystal structure of *trans*-$[Fe_2(CO)_4\{\mu\text{-}O{=}C\text{-}C(Ph){=}CH_2\}(\mu\text{-}PCy_2)(\mu\text{-}dppm)]$ 4

As discussed previously, the only isolated product from the reaction of **1b** and phenylethyne is *trans*-$[Fe_2(CO)_4(\mu\text{-}HC{=}CHPh)(\mu\text{-}PCy_2)(\mu\text{-}dppm)]$ **3a**, which was isolated in moderate yields. Close inspection of the ^{31}P NMR spectrum of the crude reaction mixture, however, revealed the presence of at least one other species and we wondered if this might be the putative α-substituted complex *trans*-$[Fe_2(CO)_4(\mu\text{-}PhC{=}CH_2)(\mu\text{-}PCy_2)(\mu\text{-}dppm)]$ **3b**. Thermolysis of the crude reaction mixture in toluene for 3 h did not appear to have any effect upon the constitution of the mixture and, in a separate experiment, **3a** was shown to be completely stable under these conditions. Chromatography of the

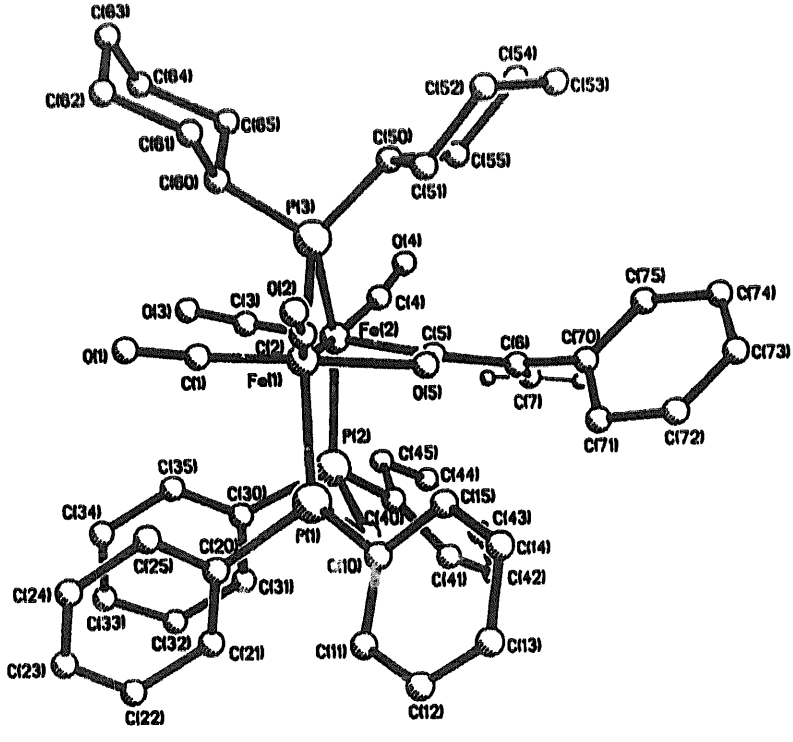

Fig. 2. Molecular structure of 4.

Table 7
Selected bond lengths (Å) and angles (°) for 4

Fe(1)-Fe(2)	2.637(3)	Fe(1)-P(1)	2.257(5)
Fe(2)-P(3)	2.232(5)	Fe(1)-P(3)	2.221(5)
Fe(2)-P(3)	2.233(5)	Fe(1)-C(1)	1.726(15)
Fe(1)-C(2)	1.732(16)	Fe(2)-C(3)	1.761(18)
Fe(2)-C(4)	1.738(16)	Fe(2)-C(5)	1.945(16)
Fe(1)-O(5)	1.991(9)	C(5)-O(5)	1.281(16)
C(5)-C(6)	1.513(21)	C(6)-C(7)	1.316(21)
Fe(1)-O(5)-C(5)	104.5(9)	Fe(2)-C(5)-O(5)	115.9(10)
Fe(1)-P(3)-Fe(2)	72.6(2)	P(1)-Fe(1)-P(3)	153.6(2)
P(2)-Fe(2)-P(3)	143.3(2)	C(1)-Fe(1)-O(5)	166.6(5)
C(2)-Fe(1)-O(5)	97.9(6)	C(3)-Fe(2)-C(5)	173.0(6)
C(4)-Fe(2)-C(5)	95.6(7)	O(5)-C(5)-C(6)	113.7(13)
C(5)-C(6)-C(7)	121.9(14)	C(5)-C(6)-C(70)	120.1(12)
C(7)-C(6)-C(70)	118.0(14)		

reaction mixture, however, revealed the presence of a small amount of a previously unobserved complex subsequently identified as the α,β-unsaturated acyl complex *trans*-$[Fe_2(CO)_4\{\mu\text{-}O{=}C\text{-}C(Ph){=}CH_2\}(\mu\text{-}PCy_2)(\mu\text{-dppm})]$ **4**. Identification was made primarily on the basis of a single crystal X-ray diffraction study, the results of which are given in Fig. 2 and Table 7.

The molecule has a *trans* arrangement of diphosphine and phosphido bridge ligands which bridge the iron–iron bond [Fe(1)–Fe(2) 2.637(3) Å] approximately symmetrically. Lying *cis* to both is an α,β-unsaturated acyl ligand which bridges the two iron atoms such that one metal is bound to oxygen [Fe(1)–O(5) 1.991(9) Å] and the second to carbon [Fe(2)–C(5) 1.945(16) Å]. The C–O bond length of 1.281(16) Å is typical of related bridging acyl complexes [9]. That there is little electron delocalisation over the vinyl portion of the acyl bridge is shown by the quite different carbon–carbon bond lengths [C(5)–C(6) 1.513(21); C(6)–C(7) 1.316(21) Å; Δ 0.197 Å] associated with localised single and double bonds respectively. This is in accordance with the bonding found in $[Fe_2(CO)_6\{\mu\text{-}O{=}C\text{-}C(OEt){=}CH_2\}(\mu\text{-}S^tBu)]$ (Δ 0.167 Å) [10], but differs from that in $[Fe_2(CO)_6\{\mu\text{-}O{=}C\text{-}CH{=}CPh(NPhH)\}(\mu\text{-}PPh_2)]$ [11], where the two carbon–carbon bonds are equidistant (1.43 Å). It should, however, be noted that the structure of the latter was of poor quality and thus its accuracy is questionable. However, in the closely related diruthenium complex $[Ru_2(CO)_6\{\mu\text{-}O{=}C\text{-}CH{=}CPh(NEt_2)\}(\mu\text{-}PPh_2)]$ [11] the formally carbon–carbon double bond at 1.394(6) Å is significantly elongated, while the nitrogen–carbon bond at 1.334(7) Å is quite short. Thus it appears that in these 3-amino-substituted complexes significant electron delocalisation occurs, a facet that is not found in **4** and other complexes such as $[Fe_2(CO)_6\{\mu\text{-}O{=}C\text{-}C(OEt){=}CH_2\}(\mu\text{-}S^tBu)]$ [10] which are not substituted in this position.

The vinyl portion of the acyl bridge is substituted at the α-position by a phenyl group which is twisted out of

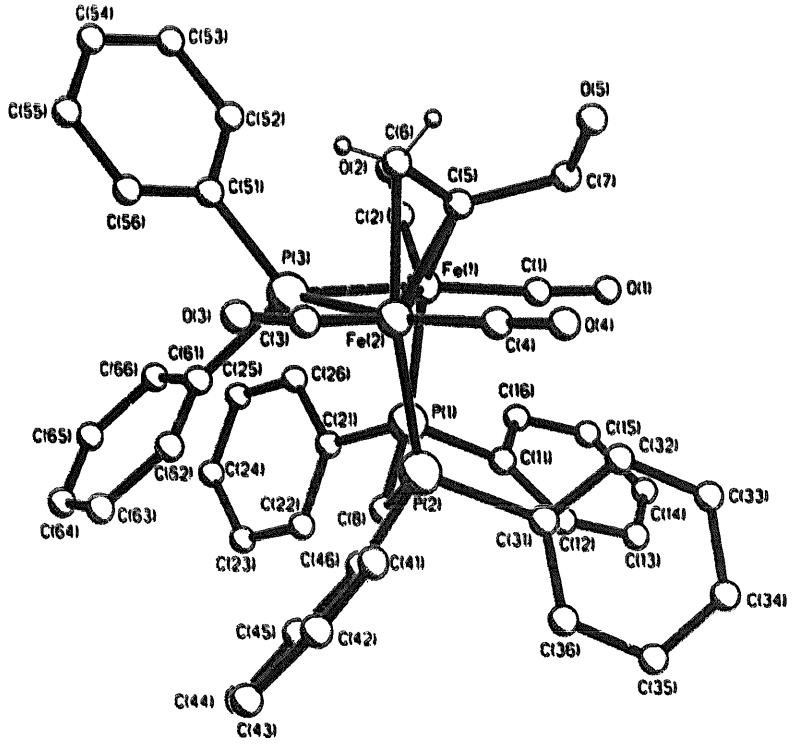

Fig. 3. Molecular structure of **5a**.

the plane of the backbone atoms. While the precise mode of formation of **4** is not known, in light of this α-substitution it is tempting to suggest that it results from CO insertion into the alkenyl ligand of the putative complex *trans*-$[Fe_2(CO)_4(\mu\text{-}PhC{=}CH_2)(\mu\text{-}PCy_2)(\mu\text{-}dppm)]$ **3b**. The CO required for the transformation presumably results from the degradation of another iron carbonyl complex. Seyferth and coworkers [10,12] have prepared a number of related thiolate-bridged complexes and report that they slowly lose CO, converting to the μ-alkenyl complexes. Phosphido-bridged α,β-unsaturated acyl complexes do not appear to undergo such rapid CO loss [11], and indeed **4** appears to be quite stable even in solution.

3.3. Reactions of 1a–b with propargyl alcohol: X-ray crystal structure of cis-$[Fe_2(CO)_4\{\mu\text{-}C(CH_2OH){=}CH_2\}(\mu\text{-}PPh_2)(\mu\text{-}dppm)]$ 5a

Room temperature reaction of **1a** with a slight excess of propargyl alcohol resulted after chromatographic separation in the isolation of *cis*-$[Fe_2(CO)_4\{\mu\text{-}C(CH_2OH){=}CH_2\}(\mu\text{-}PPh_2)(\mu\text{-}dppm)]$ **5a** and *trans*-$[Fe_2(CO)_4\{\mu\text{-}HC{=}CH(CH_2OH)\}(\mu\text{-}PPh_2)(\mu\text{-}dppm)]$ **5b** in yields of 23 and 31% respectively. The relative orientations of the bridging ligands was apparent from an analysis of phosphorus–phosphorus coupling constants to the low field phosphido resonances in the ^{31}P NMR spectra [**5a**, *J* 47, 24; **5b**, *J* 84 Hz]. The nature of **5b** was further elucidated by ^1H NMR spectroscopy, the room temperature appearance of a broad multiplet at δ 6.50, indicative of an α-carbon bound proton, revealing its identity as a β-substituted alkenyl complex. For **5a**, signals at δ 2.20 and 2.00, chemical shifts indicative of β-carbon bound protons, suggested an α-substituted product. In order to then determine the precise structure, a single crystal X-ray diffraction study was carried out, the results of which are summarised in Fig. 3 and Table 6.

The molecule has the same gross structural features as both the α-phenyl (**2a**) and α-methyl [2] derivatives, namely a *cis* arrangement of phosphorus-containing ligands and an α-substituted alkenyl ligand. The iron–iron bond length at 2.653(2) Å is indistinguishable from those in the aforementioned complexes, while similar degrees of asymmetry are seen in the iron–phosphorus bonds. Perhaps the most noteworthy difference between **2a** and **5a** is the binding of the alkenyl ligand. Thus, in **5a** C_α is bound more symmetrically to the diiron centre [Fe(1)–C_α 2.019(9); Fe(2)–C_α 2.118(10) Å; Δ 0.099 Å] than in **2a** (Δ 0.158 Å) and *cis*-$[Fe_2(CO)_4(\mu\text{-}MeC{=}CH_2)(\mu\text{-}PPh_2)(\mu\text{-}dppm)]$ (Δ 0.122 Å) [2]. More differences are seen in the binding of C_β, which lies 2.154(10) Å from Fe(2) in **5a** compared with 2.141(9) Å in **2a**. Thus in the latter, Fe(2) lies closer to C_β than C_α by 0.015 Å, while in **5a** the reverse is found, such that C_α lies closer by 0.036 Å, and in *cis*-$[Fe_2(CO)_4(\mu\text{-}MeC{=}CH_2)(\mu\text{-}PPh_2)(\mu\text{-}dppm)]$ it is bound essentially symmetrically (Δ 0.002 Å) [2].

The reaction of **1a** with propargyl alcohol closely mirrors that with phenylethyne, the major difference being that in the former case isomers were separable by column chromatography. Somewhat more contrastingly, reaction of **1b** with propargyl alcohol led, after chromatography, to the isolation in 66% yield of an inseparable mixture of α- and β-substituted isomers *trans*-$[Fe_2(CO)_4\{\mu\text{-}C(CH_2OH){=}CH_2\}(\mu\text{-}PCy_2)(\mu\text{-}dppm)]$ **6a** and *trans*-$[Fe_2(CO)_4\{\mu\text{-}HC{=}CH(CH_2OH)\}(\mu\text{-}PCy_2)(\mu\text{-}dppm)]$ **6b** in a 1:4 ratio. That both contained a *trans* arrangement of phosphorus-containing ligands was easily established from the relatively large values of phosphorus–phosphorus coupling constants [**6a**, *J* 79; **6b**, *J* 77 Hz]. In the ^1H NMR spectrum, resonances due to **6a** were difficult to discern, however, the observation of a low field multiplet at δ 6.28 associated with **6b** confirmed that this complex was the β-substituted isomer. The course of the reaction of **1b** with propargyl alcohol closely follows that with propyne [5], in which a mixture of α- and β-substituted *trans* isomers was also produced. The α:β ratio in the latter case of 2.5:1, however, differs from that seen here (1:4), while with phenylethyne (see above) the α-substituted isomer is not observed. This lends further support to our previous supposition [5] that the regioselectivity is sensitive to the steric demands of the substituent, such that Markovnikov addition which yields α-alkenyls is electronically favoured, while an increase in steric bulk of the alkyne (Ph > CH_2OH > CH_3) favours anti-Markovnikov addition, affording β-substituted products.

All alkenyl complexes formed upon insertion of propargyl alcohol are fluxional on the NMR timescale, the 'windshield-wiper' process being conveniently monitored by variable temperature ^{31}P NMR spectroscopy. Free energies of activation for the processes were calculated at 59 ± 1, 53 ± 1 and 54 ± 1 kJ mol^{-1} for **5a** (343K), **5b** (295K) and **6b** (293K) respectively, however, due to the instability of **6a** at elevated temperatures we were unable to determine its coalescence temperature. A comparison of values for **5b** and **6b** reveals that the changes in steric and electronic nature of the phosphido bridge have little effect upon the σ–π alkenyl fluxionality. There is, however, a significant difference between the free energies for isomeric **5a** and **5b** (6 kJ mol^{-1}), yet it is nowhere near as large as that, 18 kJ mol^{-1}, between **2a** and **2b**. Specifically, there is a large difference in free energy of activation for the two β-substituted complexes **2b** and **5b**. In the absence of structural data for the latter it is difficult to unambiguously assign the reason for this; however, since both Ph and CH_2OH substituents are capable of stabilising the development of positive charge at the β-carbon, ground

state structural differences cannot be ruled out. Also noteworthy in the series of complexes *cis*-[$Fe_2(CO)_4$(μ-RC=CH_2)(μ-PPh_2)(μ-dppm)], as the binding of C_α to the diiron centre becomes more symmetric (Δ), the free energy of activation for the alkenyl fluxionality decreases [R = Ph, Δ 0.158 Å, $\Delta G^{\#}$ 63 ± 1 kJ mol^{-1}; R = Me, Δ 0.122 Å, $\Delta G^{\#}$ 61 ± 2 kJ mol^{-1} (the coalescence temperature is approximately 353 K, although due to conversion to other species at this temperature the error is higher); R = CH_2OH, Δ 0.099 Å, $\Delta G^{\#}$ 59 ± 1 kJ mol^{-1}]. This again suggests that the activation energy may be highly sensitive to ground state conformation of the alkenyl ligand. Further, for both electron-releasing (Me, CH_2OH) and -withdrawing (Ph) substituents the free energies of activation for the 'windshield-wiper' fluxionality are higher for α- than for β-substituted alkenyl complexes.

Acknowledgements

We would like to thank the UCL Access Fund for a postgraduate award to M.H.L. and Professor A.J. Carty and Dr. J. Corrigan for providing samples of [$Fe_2(CO)_6$(μ-PhC=CH_2)(μ-PPh_2)] and [$Fe_2(CO)_6$(μ-HC=CHPh)(μ-PPh_2)].

References

[1] J. Boothman and G. Hogarth, *J. Organomet. Chem.*, *437* (1992) 201.
[2] G. Hogarth and M.H. Lavender, *J. Chem. Soc., Dalton Trans.*, (1992) 2759.
[3] G. Hogarth and M.H. Lavender, *J. Chem. Soc., Dalton Trans.*, (1993) 143.
[4] G. Hogarth and M.H. Lavender, *J. Chem. Soc., Dalton Trans.*, (1994) 3389.
[5] G. Hogarth, M.H. Lavender and K. Shukri, *Organometallics*, *14* (1995) 2325.
[6] G.M. Sheldrick, SHELXTL-PLUS, *Program Package for Structure Solution and Refinement*, Vers. 4.2, Siemens Analytical Instruments Inc., Madison, WI, 1990.
[7] J.R. Shapley, S.I. Richter, M. Tachikawa and J.B. Keister, *J. Organomet. Chem.*, *94* (1975) C43; L.J. Farrugia, Y. Chi and W.-C. Tu, *Organometallics*, *12* (1993) 1616 and references cited therein.
[8] S.A. MacLaughlin, S. Doherty, N.J. Taylor and A.J. Carty, *Organometallics*, *12* (1992) 4315.
[9] Y.-F. Yu, J. Gallucci and A. Wojcicki, *J. Am. Chem. Soc.*, *105* (1983) 4826; R.P. Rosen, J.B. Hoke, R.R. Whittle, G.L. Geoffroy, J.P. Hutchinson and J.A. Zubieta, *Organometallics*, *3* (1984) 846.
[10] D. Seyferth, J.B. Hoke, J.C. Dewan, P. Hofmann and M. Schnellbach, *Organometallics*, *13* (1994) 3452.
[11] G.N. Mott, R. Granby, S.A. MacLaughlin, N.J. Taylor and A.J. Carty, *Organometallics*, *2* (1983) 189.
[12] D. Seyferth, C.M. Archer, D.P. Ruschke, M. Cowie and R.W. Hilts, *Organometallics*, *10* (1991) 3363.